149 (2018) 1–13

Contents lists available at ScienceDirect

journal homepage:

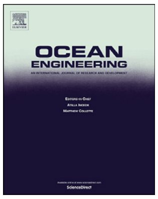

Joint experiments of cavitation jet: High-speed visualization and erosion test

Chi Peng, Shouceng Tian, Gensheng Li*

State Key Laboratory of Petroleum Resources and Engineering, China University of Petroleum-Beijing, 18 Fuxue Road, Changping, Beijing, 102249, China

ARTICLE INFO

Article history:
Received 19 July 2017
Received in revised form
3 October 2017
Accepted 5 November 2017

Keywords:
Cavitation jet
High-speed visualization
Proper Orthogonal Decomposition
Erosion test
Laser microscope

ABSTRACT

Cavitation is a ubiquitous phenomenon in ocean engineering. In order to figure out the relationship between cavitation cloud and cavitation erosion, high-speed visualization and erosion test of cavitation jet were simultaneously performed. The temporal and spatial distributions of cavitation cloud was analyzed using Proper Orthogonal Decomposition (POD) and the morphology of eroded specimen was analyzed from both macroscopic and microcosmic perspectives. The results show that POD modes of side view images are able to estimate the maximum radial distribution of cavitation pits, while the energy fraction of the first POD mode can serve as an indicator of specimen mass loss. The intensity of cavitation erosion is decided by both the bubble concentration and collapse intensity at specimen surface. At a medium standoff distance, where collapse intensity and bubble concentration are well compromised, maximum cavitation erosion is achieved. The aggravation of cavitation erosion is the combined consequences of the growth of single cavitation pits and the connection of adjacent pits. These results suggest that the collapse of cavitation bubbles is a necessary, but not sufficient, condition for severe cavitation erosion. The findings are expected to improve the physical understanding of the relationship between cavitation phenomenon and cavitation damage.

1. Introduction

Cavitation is a common phenomenon in ocean engineering, which was firstly observed by Reynolds (1894) and gained growing attention after Parsons and Cook (1919) recognized it as the source of severe erosion of warship propellers. Cavitation happens when vapor cavities, called cavitation bubbles, are formed in liquid. This is realized by dropping local pressure below saturated vapor pressure (Crum, 1982; Mørch, 2009). When subjected to high pressure, cavitation bubble collapses, generating extremely high local pressure and temperature up to several GPa and thousands of K (Alehossein and Qin, 2007; Choi and Chahine, 2016; Franc et al., 2011). If a cavitation bubble collapses close enough to a solid wall, it will induce high-speed micro-jet and shock waves (Benjamin and Ellis, 1966; Minsier et al., 2009; Momma and Lichtarowicz, 1995; Tomita and Shima, 1986), which can cause permanent deformation, pits or craters at material surface once their aggressiveness exceeds the threshold decided by material properties (Choi et al., 2014; Hsiao et al., 2014; Pöhl et al., 2015). Marine equipment such as rudder and propeller are typical parts that suffer from cavitation damage. Cavitation can also cause noise, vibration and low efficiency in fluid machinery (Arndt, 1981).

Although cavitation is not welcomed in most of engineering situations, cavitation jet that takes advantage of the energy of cavitation bubble collapse has enjoyed extensive researches and applications since 1980s. Cavitation is firstly induced in nozzle throat where local pressure drops dramatically due to Bernoulli's Principle. Microscopic roughness of nozzle inner surface, small solid impurities and dissolved gases in the liquid provide sites for heterogeneous nucleation (Holl, 1970; Mørch, 2007). Cavitation bubbles travel with water jet and then expand in shear layer where turbulent pressure can be very low, forming coalesce called cavitation cloud. As cavitation bubbles approach the target, local pressure will recover and bubbles will collapse at target surface, leading to cavitation damage. It has been proven that cavitation jet can clean the underwater pipelines of offshore oil platforms, improve drilling rate of petroleum wells (Gensheng et al., 2005; Johnson et al., 1984), and perform shotless peening (Soyama et al., 2011) et al.. It also serves as an efficient way to decide material's resistance to cavitation erosion (G134-95, 2006).

---

* Corresponding author.
E-mail addresses: 2014312018@student.cup.edu.cn (C. Peng), tscsydx@163.com (S. Tian), ligs@cup.edu.cn (G. Li).

https://doi.org/10.1016/j.oceaneng.2017.11.009
0029-8018/

Among the researches on cavitation jet, there are two popular ways: erosion test and high-speed visualization. Erosion test focuses on the mass loss, damage pattern and failure mechanism of test samples. Many researches have been done concerning the effects of relevant factors on the erosion results of cavitation jet (Chahine and Courbiere, 1987; Hattori et al., 2006; Hutli et al., 2016, 2017; Kim et al., 2014; Li et al., 2016, 2017; Soyama, 2013; Soyama and Lichtarowicz, 1998; Watanabe et al., 2016; Yamaguchi and Shimizu, 1987; Yamauchi et al., 1995), including nozzle geometry, upstream pressure, standoff distance, cavitation number, fluid temperature et al.. The double peaks of mass loss along standoff distance and ring-shape distribution of spherical cavitation pits were recognized as representative features of cavitation jet. On the other hand, high-speed visualization directly observes the cavitation cloud in cavitation jet. Collapse of cavitation cloud is closely related to cavitation erosion. High-speed photography was firstly adopted by Chahine et al. (1987), who found there was periodic shedding of cavitation cloud in cavitation jet. A typical cycle of cavitation cloud contains four stages: inception, transition, shedding and collapse. Hydraulic conditions such as upstream pressure and cavitation number would affect the size and shedding frequency of cavitation cloud. Afterwards, Soyama et al. (1995) used high-speed photography to visualize cavitation jet from conical, cylindrical and horn nozzles. They observed that the shedding frequency of cavitation cloud decreased, while the maximum length of cavitation cloud increased, with upstream pressure. Hutli and Nedeljkovic (2008) agreed on the inverse relationship between upstream pressure and shedding frequency. Nishimura et al. (2012) decided the similarity law between shedding frequency and hydraulic conditions by high-speed visualization. Wright et al. (2013) investigated the size, traveling distance, shedding frequency and front velocity of cavitation cloud under different Reynolds numbers. Utilizing frame difference method, Sato and cooperators (Hayashi and Sato, 2014; Saito and Sato, 2006; Sato et al., 2009a) argued that the reentrant jet formed by the downstream cavitation cloud collapse was responsible for the shedding of cavitation cloud issued from horn-type nozzle. This theory that re-entrant jet periodically pinches off cavitation cloud at nozzle exit was accepted by some researches (Stanley et al., 2011, 2014; Watanabe et al., 2016), and it is very similar to the cavitation cloud shedding mechanism above hydrofoils (Dular et al., 2005).

Recently, there were attempts to find the link between the behavior of cavitation cloud and cavitation erosion. Several pioneering works have been done. Dular et al. (2004) conducted optical observation of cavitation structures above hydrofoils and an obvious correlation between cavitation structures and cavitation erosion was found. The position and distribution of pits on hydrofoil surface correlated to the distribution of the images' standard deviation of gray level. Later on, Petkovšek and Dular (2013) presented a study about simultaneous observations of cavitation structures and cavitation erosion. Besides demonstrating the cause and effect between cavitation cloud collapse and cavitation erosion, they also found that the topology of cavitation cloud before collapse played a major role in erosion. In cavitation jet, Watanabe et al. (2016) experimentally studied the variations of cavitation cloud structure and erosion characteristics. They found the erosion distribution on specimen can be reproduced in the time-difference images of the cavitation cloud shadowgraphs. Hutli et al. (2017) proved that the distribution of cavitation bubble collapse at sample surface well matched the area of ring-shape erosion.

However, previous works about cavitation jet (Hutli et al., 2016, 2017; Sato et al., 2013; Soyama, 2005; Watanabe et al., 2016) usually used a couple of images from one or two cycles to represent the global behavior of cavitation cloud, which we think is defective. Although cavitation cloud has an obviously periodic behavior, they does not behave exactly the same in different cycles in terms of size and duration. In most experiments plunger pumps were used to provide upstream pressure, and the fluctuation of pump pressure cannot be avoid (Wright et al., 2013). Thus cavitation cloud appears differently in high-pressure and low-pressure phases (Peng et al., 2016; Sato et al., 2013). To accurately reflect the spatial distribution of cavitation cloud, it is necessary to introduce an approach that contains statistical ideas. In present study, Proper Orthogonal Decomposition (POD) was used.

POD is a method that can distinguish spatial and temporal coherent structures in flow field. It decomposes a time series of vector or scalar field into a set of basic spatial modes and temporal coefficients (Chatterjee, 2000; Holmes et al., 1998). POD enjoys applications in many domains such as data compression, signal analysis, image processing and fluid mechanics (Berkooz et al., 1993; Chen et al., 2012; Fogleman et al., 2004; Watanabe et al., 2015a). Recently, POD was introduced to the study of cavitation flow. Utturkar et al. (2005) applied POD to characterize the difference between cavitation models. Danlos et al. (2014) proposed to use energy fraction of the second POD mode to distinguish different cavitation regimes in a convergent-divergent nozzle. Prothin et al. (2016) highlighted the spatial and temporal behavior of cavitation cloud on a hydrofoil at high Reynolds number using POD. For cavitation jet, Watanabe et al. (2015b) obtained the spatial modes showing cavitation cloud distribution. It was found that cavitation cloud resided around center jet in an axisymmetric manner.

This paper is going to address the temporal and spatial characteristics of cavitation cloud, the erosion ability of cavitation jet, and the relationship between the two. It is hoped that present work can improve the physical understanding of the cavitation phenomenon and cavitation damage of cavitation jet. The experimental setup and data processing method are detailed in section 2. Section 3 is devoted to the presentation of the results and analysis: periodic behavior of cavitation cloud, POD results, cavitation noise, erosion patterns and their correlations.

2. Material and methods

2.1. Test rig and experiment conditions

The joint experiments of high-speed observation and erosion test were carried out at High-pressure Water-jet Laboratory of China University of Petroleum, Beijing. The test rig is schematically depicted in Fig. 1(a). A high-pressure plunger pump (KMT Streamline SL-V50) with an inbuilt bladder accumulator provided the upstream pressure, which could be read from a pressure gauge (accuracy ±0.3%FS) at pump outlet. The pressure loss along the pipelines was ignored. A turbine flowmeter (accuracy ±0.5%FS) was used to measure the flow rate. A cylindrical nozzle (Fig. 1(b)) was used, with throat diameter of 0.3 mm. A cylindrical water vessel made of transparent acrylic resin, with diameter of 35 cm and height of 25 cm, was used to produce submerge condition. The lateral and axial coordinates x and y were defined, with the origin set at the nozzle exit. Standoff distance y can be adjusted at a resolution of 0.1 mm, and the non-dimensional standoff distance (NSD) is defined as $y/throat\ diameter$.

In all experiments, upstream pressure was set at 50 MPa. Flow rate was 0.96 ± 0.05 L/min. Nozzle discharge coefficient was about 0.71. Cavitation number $\sigma = (P_{downstream} - P_{vapour})/0.5\rho V_{throat}^2$ is 0.038. Standoff distances ranging from 2.5 to 60 mm (NSD 8.3–200) were investigated. Tap water was used and additional cold water was injected to the vessel through a tube with diameter